Biosensors and Bioelectronics 74 (2015) 454–460

Contents lists available at ScienceDirect

Biosensors and Bioelectronics

journal homepage: www.elsevier.com/locate/bios

A polydopamine-modified optical fiber SPR biosensor using electroless-plated gold films for immunoassays

Se Shi [a], Libing Wang [a,d], Rongxin Su [a,b,*], Boshi Liu [a,b], Renliang Huang [c], Wei Qi [a,b], Zhimin He [a]

[a] State Key Laboratory of Chemical Engineering, School of Chemical Engineering and Technology, Tianjin University, Tianjin 300072, China
[b] Collaborative Innovation Center of Chemical Science and Engineering (Tianjin), Tianjin 300072, China
[c] School of Environmental Science and Engineering, Tianjin University, Tianjin 300072, China
[d] Research Center of Hunan Entry–Exit Inspection and Quarantine Bureau, Changsha 410001, China

ARTICLE INFO

Article history:
Received 26 March 2015
Received in revised form
24 June 2015
Accepted 30 June 2015
Available online 2 July 2015

Keywords:
Electroless plating
Optical fiber SPR biosensor
Polydopamine
Surface functionalization
Antibody immobilization
Immunoassays

ABSTRACT

A sensitive and stable electroless-plated gold film for the preparation of an optical fiber surface plasmon resonance (SPR) sensor is presented in this work, together with a facile antibody immobilization method. Gold nanoparticles were uniformly adsorbed onto the surface of an optical fiber forming a film with a thickness of approximately 56.3 nm. The sensor had a high sensitivity with 2054 nm/RIU and 3980 nm/RIU in the refractive index ranges of 1.333–1.359 and 1.359–1.386, respectively. An SPR biosensor was developed based on polydopamine-modified gold film (PDA-Au), which was fabricated by a simple and quick spontaneous polymerization of dopamine (DA) on the gold film. When goat anti-human IgG antibodies were immobilized, the PDA-Au surface had a larger resonant wavelength shift of 66.21 nm compared with the traditional 11-mercaptoundecanoic acid-modified gold film (MUA-Au) surface. In addition, the PDA-Au surface enabled the sensitive and selective determination of human IgG down to a concentration of 2 μg mL^{-1} with a high sensitivity of 0.41 nm per μg mL^{-1}. The PDA-Au surface exhibited an approximately four fold higher sensitivity and an about seven fold lower LOD than the MUA-Au surface to human IgG.

1. Introduction

Optical fiber surface plasmon resonance (SPR) biosensors are usually applied to analyze molecular interactions and determine the concentration of the target molecule. These biosensors have been widely applied in various areas, such as disease diagnosis (Perez-Ruiz et al., 2014; Zhao et al., 2015), DNA hybridization and cellular behavior monitoring (Pollet et al., 2009; Shevchenko et al., 2014), as well as environmental and food safety determinations (Verma and Gupta, 2015; Wang et al., 2013). These biosensors not only retain the advantages of prism SPR biosensors, including that they have a high sensitivity, are label-free, are non-destructive and allow for real-time detection, but they also possess unique features such as miniaturization, flexibility, resistance to electromagnetic interference and a remote sensing capability (Sharma et al., 2007). However, there are two challenges during their fabrication and application. First, the preparation of the optical fiber SPR sensor requires some special rotation devices in the vacuum evaporation or sputtering systems, ensuring that the deposition of gold films on the cylindrical optical fiber surface is as uniform as possible. Its preparation is more difficult than the preparation of the prism SPR sensor, during which the metal is simply deposited on the planar glass slide. Secondly, more effective methods for the immobilization of functional molecules are still required, which can provide more binding sites for the target molecules and thus achieve a higher sensitivity during the SPR analysis.

A uniform thin metal film is essential to the high sensitivity and perfect spectroscopic profile of the SPR sensor. Generally, SPR-active films are prepared by vacuum evaporation or sputtering of the metals using expensive and complicated equipment. However, to ensure that the film around the curved surfaces of the optical fiber has a uniform thickness, specific rotation devices (Navarrete et al., 2010; Suzuki et al., 2008; Zhao et al., 2014) are required in the vacuum coating techniques. As another option for applying the metal nanofilm coating, electroless plating (ELP) is based on the chemical reduction of metal ions to deposit the metal onto the substrate. Recently, ELP has drawn great attention in the fabrication of microelectrodes (Flavel et al., 2009; Honda et al., 2005), signal amplification (Kim and Lee, 2012; Tabakman et al., 2011;

* Corresponding author at: State Key Laboratory of Chemical Engineering, School of Chemical Engineering and Technology, Tianjin University, Tianjin 300072, China. Fax: +86 22 27407599.
E-mail address: surx@tju.edu.cn (R. Su).

http://dx.doi.org/10.1016/j.bios.2015.06.080
0956-5663/

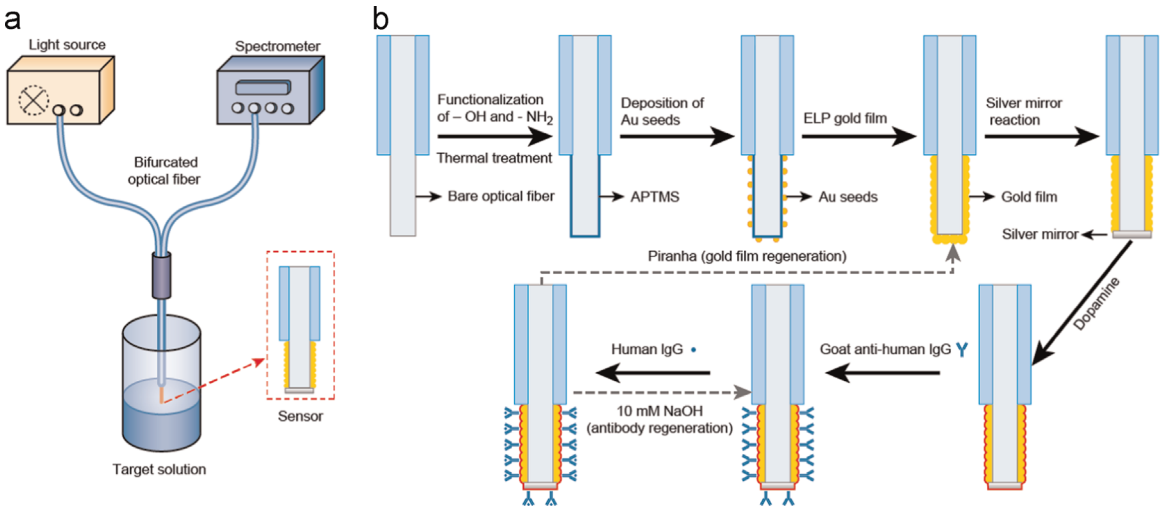

Fig. 1. (a) Schematic diagram of the measurement system using the optical fiber SPR sensor. (b) Illustration of the ELP fabrication and PDA-modification of gold films for IgG immunoassay.

Yang et al., 2014) and catalysts (Muench et al., 2012). Compared with vacuum deposition, ELP has many advantages. First, it does not require any expensive or complicated equipment, and it is easy to perform in common laboratories. Secondly, the negative effect of the Cr on the SPR plasma properties can be avoided by using chemicals as coupling agents. Lastly, but most importantly, it can provide uniform surface coverage on multidimensional surfaces without the directional limitation encountered during evaporation or sputtering (Zabetakis and Dressick, 2009). Therefore, ELP is more appropriate than vacuum deposition for the formation of films on the optical fiber.

The immobilization of antibodies on the biosensor surface plays an important role in the performance of the SPR immunoassay. The more effective the antibody immobilization is, the more antigens will be detected. Many methods, such as linking amine groups to the 1-ethyl-3-(3-(dimethylamino)propyl)-carbodiimide hydrochloride/N-hydroxysulfosuccinimide (EDC/NHS) activated carboxyl group (Liu et al., 2014b), connecting biotin to avidin, using protein A (Ko et al., 2009) or protein G (Maisonneuve et al., 2015) as a sub-layer protein, have been employed to immobilize the antibodies. Dopamine (DA), inspired by the adhesion of mussels, can be easily deposited with a controlled film thickness on almost all of the substrates by simple self-polymerization (Lee et al., 2007). It is reported that 10 min was sufficient to achieve a topologically continuous polydopamine (PDA) film with maximum film and group coverage (Zangmeister et al., 2013). Therefore, the polymerization of DA could be a simple and quick surface functionalization method for use on SPR biosensors. Although the chemical composition of PDA is not precisely known, catechol and quinone functional groups are believed present in the polymer (Liu et al., 2014c). In slightly alkaline conditions, the reaction equilibrium shifts from the catechol to the quinone groups (Lee et al., 2006; Li et al., 2013; Lynge et al., 2011). The quinones are capable of covalent coupling to amine-terminated or thiol-terminated biomolecules by Michael addition or Schiff base reactions (LaVoie et al., 2005; Lee et al., 2009; Li et al., 2013; Wan et al., 2011). The chemical attachment of PDA has been shown to have better hydrolysis resistance compared to the standard EDC/NHS coupling of amine-terminated biomolecules to carboxylic acid-modified surfaces (Lee et al., 2009). Therefore, the polydopamine-modified gold film (PDA-Au) surface is more appropriate than the traditional 11-mercaptoundecanoic acid-modified gold film (MUA-Au) surface for the immobilization of the antibody on the SPR sensor.

In this study, we used a facile ELP method instead of the vacuum coating technique to prepare an optical fiber SPR sensor and presented an effective antibody immobilization procedure to sensitively and selectively detect human IgG. The morphology and thickness of the gold film were characterized using scanning electron microscope (SEM). The sensitivity and stability of this sensor were further investigated. In addition, the self-polymerization of DA was used to provide a simple and quick surface functionalization method for the SPR biosensor. Antibody immobilization and antigen recognition capacities of the PDA-Au biosensor were also investigated and compared to those of a MUA-Au biosensor.

2. Materials and methods

2.1. Materials

Gold (III) chloride trihydrate ($HAuCl_4 \cdot 3H_2O$), dopamine hydrochloride, 1-ethyl-3-(3-(dimethylamino)propyl)-carbodiimide hydrochloride (EDC), N-hydroxysulfosuccinimide (NHS), 11-mercaptoundecanoic acid (MUA), ethanolamine hydrochloride (EA), bovine serum albumin (BSA) and lysozyme were purchased from Sigma-Aldrich. 3-aminopropyltrimethoxysilane (APTMS), $NaBH_4$, and hydroxylamine hydrochloride ($NH_2OH \cdot HCl$) were purchased from the Sinopharm Chemical Reagent Co., Ltd. (China). Goat anti-human IgG and human IgG were purchased from the Beijing Biosynthesis Biotechnology Co., Ltd. Phosphate buffered saline (PBS, 10 mM, pH 7.4, 1.76 mM KH_2PO_4, 10.14 mM $Na_2HPO_4 \cdot 12H_2O$, 136.75 mM NaCl, 2.68 mM KCl) and Tris buffer (10 mM, pH 8.9) were prepared with ultra-pure water. All of the chemicals used were of analytical reagent grade. Multimode optical fibers with a 400 μm core diameter and a 0.22 numerical aperture were purchased from Ocean Optics Inc., USA.

2.2. Experimental setup

Fig. 1a shows the schematic diagram of the measurement system using the optical fiber SPR sensor. One end of the sensor was connected to the end of the bifurcated optical fiber (SPLIT-400-VIS-NIR, Ocean Optics), and the other end with the sensing area was immersed into the target solution. The white light emitted from a tungsten-halogen light source (DH-2000-BAL, Ocean Optics) was conducted into the sensor through the bifurcated optical

fiber. The interaction between the incident light and the sensor was used to modulate the optical signal reflected by the silver layer and captured by a mini-spectrometer (USB2000+, Ocean Optics), which was connected to the other end of the bifurcated optical fiber. The signal obtained could be shown and monitored by a computer connected with the spectrometer.

2.3. ELP preparation of the gold film for the optical fiber SPR sensor

The ELP preparation process of the gold film for the optical fiber SPR sensor was divided into four steps. In the first step, the sensing area of the optical fiber was immersed in freshly prepared piranha solution (with a ratio of 7:3 of H_2SO_4:H_2O_2) at 90 °C for 30 min, after which it was rinsed with deionized (DI) water and placed in an oven at 100 °C for 1 h. Negatively charged hydroxyl moieties were firmly generated on the optical fiber by the piranha oxidation and the thermalization that followed. Then, the sensing area was functionalized with 3-aminopropyltrimethoxysilane (APTMS) solution in methanol (10%, v/v) for 6 h, after which it was rinsed with methanol and annealed in an oven at 110 °C for 1 h. In the second step, citrate capped Au seeds (approximately 2.5 nm) synthesized by the standard citrate reduction method (Grabar et al., 1996) were adsorbed onto the APTMS-functionalized surface by immersing the optical fiber in the colloidal gold solution for 8 h. The optical fiber with Au seeds immobilized on it was rinsed with DI water, dried in a N_2 stream and immediately used in the ELP. In the third step, the optical fiber sensing area with adsorbed Au seeds was immersed in freshly prepared ELP solution (0.1% $HAuCl_4$ and 0.4 mM $NH_2OH \cdot HCl$) under shaking at 100 rpm for 7 min to form a continuous gold film. After that, the gold film was immediately rinsed with water and dried in a N_2 stream. Finally, a thin silver layer was coated onto the end surface of the gold film-coated fiber using Tollens' reagent to create the mirror that would allow the back reflection of the light in the fiber. Fig. 1b demonstrates the preparation process of the electroless-plated gold film optical fiber SPR sensor.

2.4. Immunoassay using the PDA-modified biosensor

The optical fiber SPR sensor obtained by ELP was immersed in an aqueous solution of DA (2 mg mL^{-1} of 10 mM Tris buffer, pH 8.5) under shaking at 120 rpm for 30 min at room temperature to form a PDA layer and then rinsed with DI water for further use. The PDA-coated sensor was transferred into a goat anti-human IgG antibody solution (100 μg mL^{-1} of PBS buffer). The sensor system was used to monitor the resonant wavelength shifts resulting from the adsorption of the antibodies onto the PDA-Au. After achieving adsorption equilibrium, the sensor was transferred into an incubator at 4 °C overnight for further deposition of the antibodies. After washing with PBS buffer, the antibody-immobilized sensor was used for human IgG detection. The sensor was immersed in human IgG diluted with PBS buffer at different concentrations at 37 °C for 30 min. The sensor system monitored the resonant wavelength shifts resulting from the interactions between human IgG and goat anti-human IgG antibodies. After the detection of one sample at a certain concentration, the antibody-immobilized sensor was regenerated by being immersed in 10 mM NaOH for 10 min before the next detection. Gold films could also be regenerated by being placed in the piranha solution for 1 min before the next PDA modification and immunoassay (Fig. 1b also demonstrates the biosensing approaches based on the PDA-modified electroless-plated optical fiber SPR biosensor).

To evaluate the selectivity, human IgG, BSA, BSA+human IgG, lysozyme, lysozyme+human IgG, β-lactoglobulin and β-lactoglobulin+human IgG were determined by the present method.

The MUA-Au for the immunoassay was used as a comparison experiment. The gold film sensor was immersed in a MUA ethanol solution (1 mM) at room temperature for 12 h, followed by washing with ethanol and drying under a N_2 stream. The carboxylic group of the thiolated surface was activated with an aqueous solution of a mixture of EDC/NHS (0.4 mM/0.1 mM) at room temperature for 30 min. After washing with an aqueous solution and drying, the immunoassay using MUA-Au was performed using the same processes as that of PDA-Au except for ethanolamine (1 M pH 8.5) was used to deactivate the residual NHS-activated carboxyl groups.

3. Results and discussion

3.1. Surface characterization of the sensor

The left part of the sensor is the subminiature version A (SMA) adapter used to connect the bifurcated optical fiber, and the right part is the sensing area with the shiny gold film, which was immersed in the analyte (Fig. S1a). To directly observe the surface morphology and thickness of the electroless-plated gold film, we employed SEM to characterize the samples. Fig. 2a and b show the surface and cross-section SEM images of the electroless-plated gold film. Gold nanoparticles with narrow gaps were uniformly adsorbed on the optical fiber, which formed a relatively continuous gold film with a thickness of 56.3 ± 1.6 nm. Because it was difficult to measure the contact angle on a thin cylindrical optic fiber, an electroless-plated gold film was coated onto a glass slide, on which the static water contact angle was measured to characterize the hydrophilicity of the electroless-plated films. The electroless-plated gold films exhibited a slight hydrophilicity with a contact angle of 74° (Fig. S1b). However, the sputtered-gold films had a strong hydrophobicity with a contact angle of 103°. Most likely, the electroless-plated gold films have a potentially lower protein fouling property compared with the sputtered gold films.

3.2. Sensitivity to the change in the surrounding refractive index of the sensor

In order to evaluate the sensitivity of the electroless-plated optical fiber SPR sensors to the surrounding refractive index, we immersed the sensors in various solvents (Table S1) with different refractive indexes ranging from 1.333 to 1.386 and measured their resonant wavelengths in these solutions. As shown in Fig. 2c, the SPR wavelength redshifts with an increase in the refractive index. The linear relationships between the SPR resonant wavelength and the refractive index ranges of 1.333–1.359 and 1.359–1.386 refractive index units (RIU) were observed, respectively, as displayed in Fig. 2d. The refractive index sensitivity (RIS) is defined as $S_n = \delta\lambda_{res}/\delta n_s$, where δn_s is the change in the refractive index of the solution, and $\delta\lambda_{res}$ is the shift in the corresponding resonance wavelength. The sensitivities of the electroless-plated gold film optical fiber SPR sensor to changes in the surrounding refractive index were 2054 nm/RIU and 3980 nm/RIU in the RI ranges of 1.333–1.359 and 1.359–1.386, respectively. Compared with optical fiber SPR sensors using sputtered gold films (Huang et al., 2013; Pollet et al., 2009; Suzuki et al., 2008) and optical fiber LSPR sensors (Cao et al., 2013; Liu et al., 2014a; Sciacca and Monro, 2014; Tu et al., 2014), optical fiber SPR sensors using the electroless-plated gold films exhibited between 1.3- and 10-fold improved sensitivities, and their sensitivities were as high as optical fiber SPR sensors using silver films prepared by the silver mirror reaction (Zhao et al., 2014) (Table 1).

There are some reasons for the high sensitivities of optical fiber SPR sensors using electroless-plated gold films. First, the resonant SPR wavelength (when the surrounding RI was 1.333) of the

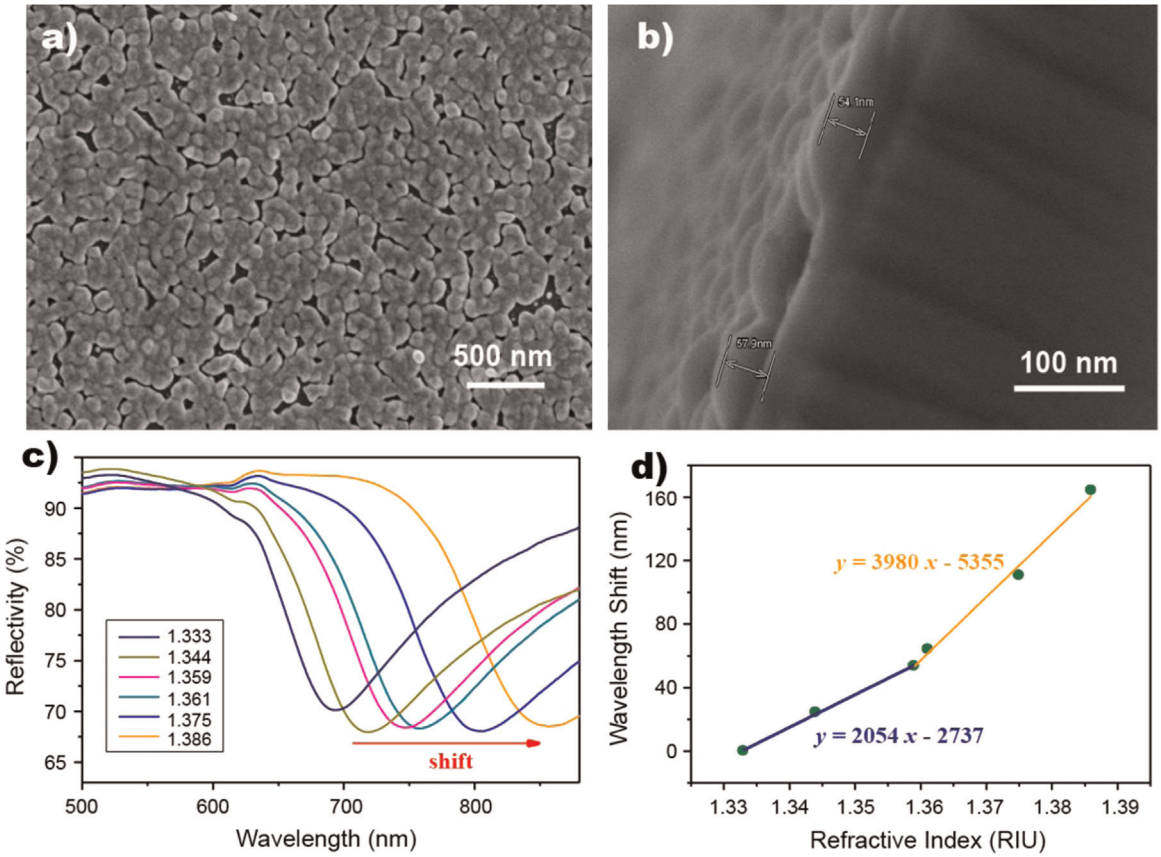

Fig. 2. SEM images of the surface (a), cross-section (b) of the electroless-plated gold film. (c) Reflectivity spectra of the electroless-plated optical fiber SPR sensor in solvents with different RI values. (d) Plot of the resonant wavelength shift (compared with RI: 1.333) vs. the RI value of the electroless-plated optical fiber SPR sensor.

Table 1
Comparison of the sensitivities of optical fiber SPR sensors prepared by different methods.

Sensor preparation method	Refractive index linear range (RIU)	Sensitivity (nm/RIU)	Reference
Sputtering gold film	1.333–1.347	1557	(Suzuki et al., 2008)
	1.333–1.354	1421	(Pollet et al., 2009)
	1.338	1090	(Huang et al., 2013)
	1.363	2613	
LSPR Au particle	1.330–1.370	387	(Sciacca and Monro, 2014)
LSPR Au rod	–	914	(Cao et al., 2013)
LSPR Au triangle	–	963	(Liu et al., 2014a)
LSPR Au cage	–	1993	(Tu et al., 2014)
Silver mirror reaction	1.333–1.352	1412	(Zhao et al., 2014)
	1.356–1.386	3906	
ELP gold film	1.333–1.359	2054	This work
	1.359–1.386	3980	

electroless-plated gold film red-shifts to near-infrared. It was reported that RIS showed a strong dependence on the wavelength of the surface plasmon maximum extinction, i.e., the gold film with a surface plasmon band at a longer wavelength exhibits a higher RIS (Karakouz et al., 2009). Secondly, optical fiber sensors using electroless-plated gold films exhibit 3D Au NPs adsorbed on the sensors, which have a larger surface area compared with the sputtered planar gold films. Such structures gave a larger fraction of the spatial region enhanced electric fields exposed to the environment and thus accessible by molecular species (Dmitriev et al., 2008; Hatab et al., 2010). Last but not the least, the gold film was composed of Au NPs (Fig. 2a), most of which were cross-linked, indicating that this sensor might be the coupling of the LSPR and SPR. It was reported that the coupling could lead to an enhanced local field and a shift in the spectral position due to the hybridization of the modes (Prodan et al., 2003).

The full width at half maximum (FWHM) of the prepared sensor was also evaluated. As shown in Fig. S2, a relatively narrow FWHM of 108.2 nm was obtained at λ=694 nm. The figure of merit (FOM=S_n/FWHM) is a widely accepted measurement for characterizing the performance of a refractive index sensor, where S_n stands for the refractive index sensitivity and FWHM is the corresponding full width at half maximum. The FOM value of the optical fiber SPR sensor using electroless-plated gold films was determined to be 19.

3.3. Adhesion and stability tests of the gold film

Good adhesion and stability of the gold film on the optical fiber are necessary in the process of its application. Here, the adhesion and stability of the gold film were qualitatively evaluated by comparing reflection spectra before and after the following treatments carried out sequentially: (1) being pressed and pulled back using a piece of Scotch tape, (2) rinsing with water and ethanol for 20 min, respectively, (3) ultrasonic treatments in water and ethanol for 10 min, respectively, (4) immersion in piranha solution for 10 min followed by a silver mirror treatment (the silver layer on the end of the sensor dissolved when the gold film was treated by the piranha, so a second silver mirror reaction was necessary for the next measurement). As shown in Fig. 3a, the reflection spectra of the sensor after all of the above treatments almost overlapped with the original one without treatment. It

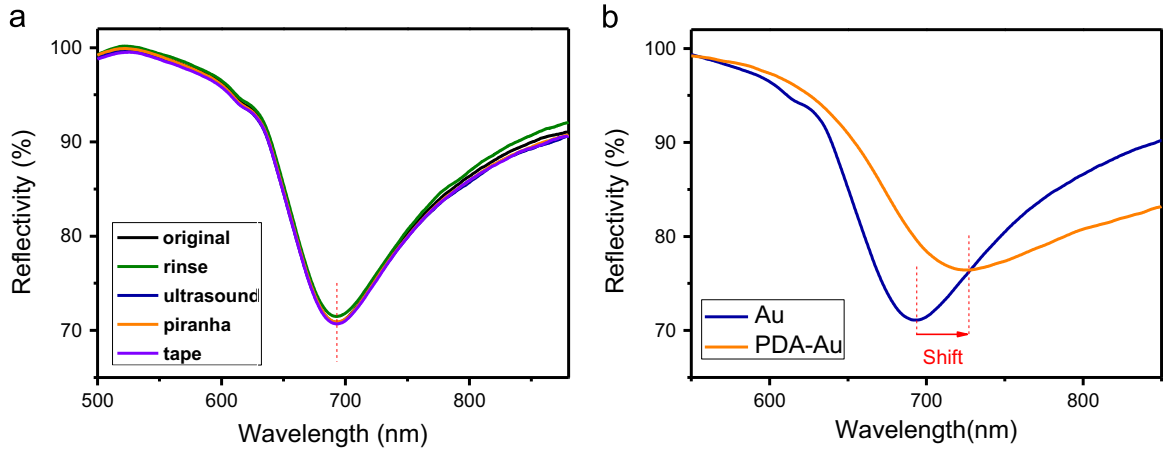

Fig. 3. (a) Reflectivity spectra of the electroless-plated optical fiber SPR sensor after the following treatment steps: before treatment; rinsing with water and ethanol; ultrasonication in water and ethanol; immersion in piranha solution and tape adhesion. (b) Reflectivity spectra of the electroless-plated optical fiber SPR biosensor before (blue line) and after (orange line) PDA modification. (For interpretation of the references to color in this figure legend, the reader is referred to the web version of this article.)

proved the excellent mechanical and chemical stability of the electroless-plated gold film. These could be attributed to the APTMS coupling with the Au NPs, thermal curing after the piranha and APTMS treatments, and storage after the films were freshly prepared.

3.4. Functionalization of the gold film and immobilization of goat anti-human IgG

In this work, the gold film was functionalized by the simple and quick spontaneous polymerization of DA onto its surface. The SPR spectra were measured before and after the polymerization to evaluate the functionalization. As shown in Fig. 3b, the resonant wavelength of the sensor shifts from 693.77 nm to 727.56 nm after the formation of the PDA layer. This result indicated that a good PDA membrane was formed on the gold film biosensor surface.

Effective antibody immobilization gives immunoassays more binding sites, which is important for antigen detection. In this work, a two-step antibody immobilization was applied for the first time in the construction of an optical fiber SPR biosensor. After the gold film was modified by PDA, it was immersed in the goat anti-human IgG (100 μg mL^{-1} in PBS buffer) to immobilize the antibodies. The Schiff base reaction between quinones in PDA and amine groups in the antibodies led to the antibodies being immobilized on the biosensor surface. A comparison experiment was done by immersing the MUA-Au activated by EDC/NHS into the antibody solution at the same concentration. As shown by the orange line in Fig. 4a, the resonant wavelength of the PDA-Au biosensor exhibited an obvious shift at first, then increased at gradually slower rates with time, and finally was almost unchanged when the time was longer than 4 h, which indicated that the immobilization of goat anti-human IgG on the sensor was accomplished. The maximum resonant wavelength shift for the antibody immobilization was 52.49 nm. As shown by the blue line, the adsorption kinetics curve of the antibody immobilization of the MUA-Au biosensor indicated that the immobilization was accomplished after 2.5 h, and the maximum resonant wavelength shift was 28.05 nm. Although the required time for equilibrium to be achieved was shorter for the MUA-Au biosensor than for the PDA-Au biosensor, the slope of both lines indicated that the PDA-Au biosensor had a quicker reaction rate than the MUA-Au biosensor.

For further antibody immobilization, this reaction continued overnight at 4 °C. As shown in Table S2, the maximum resonant wavelength shift after antibody immobilization on the PDA-Au surface was 66.21 nm, whereas the shift on the MUA-Au surface was only 30.50 nm. These results proved that the Schiff base reaction between the amine group of the antibody and the quinone group of PDA was a good method for immobilizing antibodies onto the SPR biosensor. The immobilization efficiency of the antibody

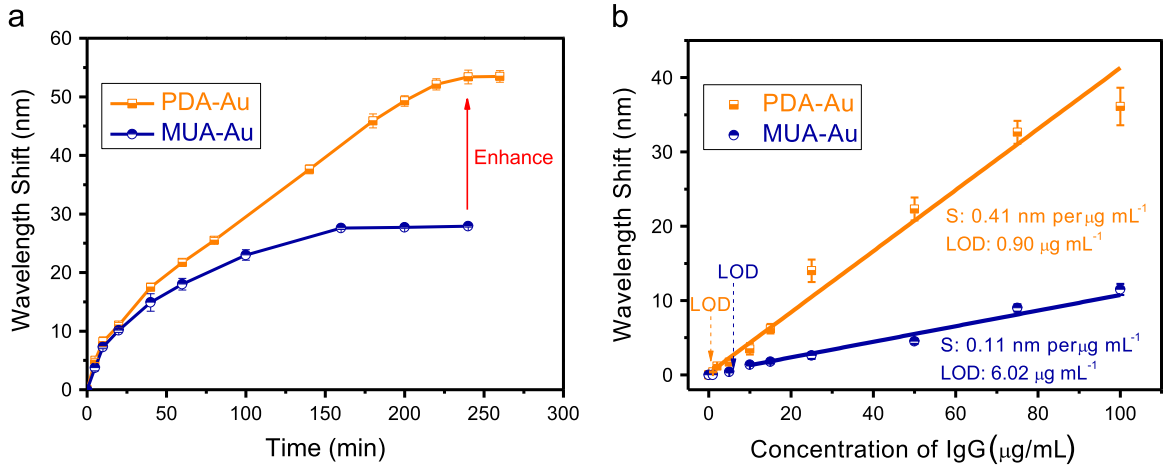

Fig. 4. (a) Kinetic absorption curves of immobilized goat anti-human IgG at the concentration of 100 μg mL^{-1} on the PDA-Au (orange line) and MUA-Au (blue line) surfaces. (b) Calibration curves for human IgG detection based on the PDA-Au (orange line) and MUA-Au (blue line) biosensors. Errors bars represent the standard deviation from three independent experiments. (For interpretation of the references to color in this figure legend, the reader is referred to the web version of this article.)

was related to both the number of binding sites and the proper space between the binding sites (Zhang et al., 2013a). First, the multilayer structure of PDA formed on the gold film resulted in more binding sites for antibody immobilization compared with the monolayer MUA on the gold film. Secondly, the PDA attachment can avoid the hydrolysis of the NHS ester compared with the standard EDC/NHS coupling of amine-terminated biomolecules to carboxylic acid-modified surfaces (Lee et al., 2009). Finally, the surface of PDA was relatively rougher because of the more abundant functional groups than the Au NP surface on the gold film, and this roughness might offer an expanded surface and less steric hindrance for antibody immobilization. Due to more binding sites and the appropriate space, it is more effective for antibodies to be immobilized on the PDA-Au surface than on the MUA-Au surface.

3.5. Sensitivity and specificity of the detection of human IgG

The goat anti-human IgG-immobilized biosensor was exposed to human IgG solutions of different concentrations to evaluate the sensitivity of the PDA-Au biosensor. A comparison experiment was done using the antibody-immobilized MUA-Au biosensor by the same method as that of PDA-Au biosensor. The shifts in the SPR resonant wavelength caused by the antibody-antigen interaction were recorded, as shown in Fig. 4b. The PDA-Au biosensor demonstrated a satisfactory linear response ($R^2=0.98$) to human IgG within the concentration range from 2 to 100 μg mL^{-1}. The sensitivity, defined as the assay response per unit of analyte concentration (the slope of the calibration curve), was estimated to be 0.41 nm per μg mL^{-1}. The limit of detection (LOD) was calculated as the concentration corresponding to the sensor signal that is equal to the mean plus three standard deviations of the background noise. The value was 0.90 μg mL^{-1} in this work. The MUA-Au biosensor demonstrated a satisfactory linear response ($R^2=0.96$) to human IgG within the concentration range from 10 to 100 μg mL^{-1}. The sensitivity and the LOD were 0.11 nm per μg mL^{-1} and 6.02 μg mL^{-1} respectively, as calculated according to the same methods as those of the PDA-Au biosensor. The PDA-Au surface exhibited an approximately four fold higher sensitivity and an about seven fold lower LOD than the MUA-Au surface to human IgG. Compared with other SPR sensors for IgG detection, the sensitivity and LOD values (0.41 nm per μg mL^{-1}, 0.90 μg mL^{-1}) of this PDA modified biosensor were close to those of the photonic crystal fiber SPR sensor (0.46 nm per μg mL^{-1}, 0.27 μg mL^{-1}) based on protein G as a sublayer (Wong et al., 2013), but much better than those of the MUA-modified SPR sensor (0.09 nm per μg mL^{-1}, 1.6 μg mL^{-1}) (Zhang et al., 2013b). The higher sensitivity could be attributed to the larger number of antibodies immobilized on the PDA-Au surface. If more antibodies are immobilized, then more antigens can be detected.

To estimate the specificity of the PDA-Au biosensor, we measured the adsorption of reference proteins (BSA, lysozyme and β-lactoglobulin) on the anti-human IgG-immobilized PDA-Au biosensor and also detected the target human IgG in multicomponent solutions including BSA+human IgG, lysozyme+human IgG and β-lactoglobulin+human IgG. As shown in Fig. 5 (solid bars), the resonant wavelength shift for only human IgG was 9.94 nm. However, the shifts of the BSA, lysozyme and β-lactoglobulin reference proteins were only 0.64 nm, 1.28 nm and 0.31 nm, respectively. The resonant wavelength shifts of the target human IgG in BSA (9.97 nm), in lysozyme (11.50 nm) and in β-lactoglobulin (10.14 nm) were very close to that of only human IgG. Using BSA, lysozyme and β-lactoglobulin as reference proteins, the signal-to-noise ratios for the target human IgG were 15.53, 7.77 and 32.06, respectively, suggesting a good selectivity for the human IgG immunoassay.

In order to evaluate the effect of the concentration of reference proteins on the specificity of the PDA-Au biosensor, we performed the specificity experiment using the higher concentration of reference proteins (100 μg mL^{-1}) than that (25 μg mL^{-1}) of reference proteins in the above experiments. As shown in Fig. 5, compared the hatched bars with the solid bars, the wavelength shifts of the anti-human IgG-immobilized PDA-Au biosensor in the high concentration of reference proteins were close to those of the biosensor in the low concentration of reference proteins, suggesting that the PDA-Au biosensor still has a good selectivity in the high concentration of reference proteins.

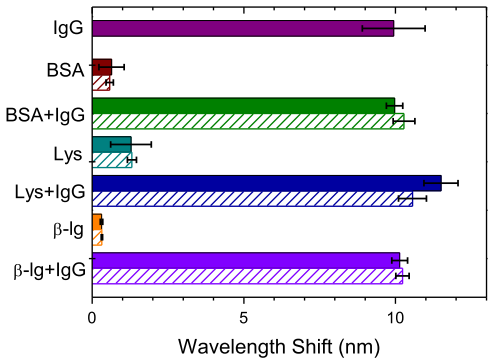

Fig. 5. Shifts of the resonant wavelength measured with different antigens (human IgG, BSA, BSA+human IgG, lysozyme, lysozyme+human IgG, β-lactoglobulin and β-lactoglobulin+human IgG) based on the PDA-Au biosensor. The concentration of human IgG was all 25 μg mL^{-1}, and the concentrations of reference proteins were all 25 μg mL^{-1} (solid bars) and 100 μg mL^{-1} (hatched bars). The errors bars represent the standard deviation from three independent experiments.

3.6. Sensor regeneration and stability

The antibody-immobilized biosensor was regenerated by being immersed in the 10 mM NaOH for 10 min, and it still kept good detection ability after five times regeneration (Fig. S4). The stability of antibody-immobilized biosensor was assessed by storing it at 4 °C in 10 mM PBS (pH 7.4) and using it to detect the 50 μg mL^{-1} human IgG after five days and ten days respectively. There was no decrease in the IgG detection response of the antibody immobilized biosensor for ten days (Fig. S5). These results indicated the good regeneration ability and stability of the antibody immobilized PDA-Au biosensor. The gold film was regenerated by being immersed in the piranha solution for 1 min followed by a silver mirror reaction on its end surface. After regeneration, the resonant wavelength of the sensor could be recovered to that of a freshly prepared sensor (Fig. S6).

4. Conclusions

We fabricated an optical fiber SPR biosensor using an electroless-plated gold film, which was composed of uniform Au NPs forming a relatively continuous construction. The prepared sensor had an excellent sensitivity compared with the reported sensors prepared by vacuum coating technology. Furthermore, the electroless-plated gold film displays good stability despite rinsing, ultrasonication, piranha solution immersion and tape adhesion treatments. In addition, an efficient antibody immobilization method was performed via a Schiff base reaction between antibodies and the PDA-functionalized gold surface. Compared with the traditional manner of antibody immobilization, in which amine groups were linked to the EDC/NHS activated carboxyl surface, this method displayed a better antibody immobilization efficiency, a higher sensitivity and a lower LOD for the detection of human IgG. Therefore, ELP and PDA have great potential in the fabrication of sensor substrates, functional modification and

biomolecule immobilization, considering the simple preparation device and the nice performance of the electroless-plated optical fiber sensor as well as the excellent antibody immobilization capacity and high sensitivity of the PDA-Au biosensor.

Acknowledgments

This work was supported by the Ministry of Science and Technology of China (Nos. 2012YQ090194, 2012AA06A303 and 2012BAD29B05), the National Natural Science Foundation of China (Nos. 51473115 and 21276192), and the Ministry of Education of China (No. B06006 and NCET-11-0372).

Appendix A. Supplementary information

Supplementary data associated with this article can be found in the online version at http://dx.doi.org/10.1016/j.bios.2015.06.080.

References

Cao, J., Tu, M.H., Sun, T., Grattan, K.T.V., 2013. Sens. Actuators B: Chem. 181, 611–619.
Dmitriev, A., Hagglund, C., Chen, S., Fredriksson, H., Pakizeh, T., Kall, M., Sutherland, D.S., 2008. Nano Lett. 8, 3893–3898.
Flavel, B.S., Yu, J., Ellis, A.V., Shapter, J.G., 2009. Electrochim. Acta 54, 3191–3198.
Grabar, K.C., Allison, K.J., Baker, B.E., Bright, R.M., Brown, K.R., Freeman, R.G., Fox, A. P., Keating, C.D., Musick, M.D., Natan, M.J., 1996. Langmuir 12, 2353–2361.
Hatab, N.A., Hsueh, C.-H., Gaddis, A.L., Retterer, S.T., Li, J.-H., Eres, G., Zhang, Z., Gu, B., 2010. Nano Lett. 10, 4952–4955.
Honda, N., Inaba, M., Katagiri, T., Shoji, S., Sato, H., Homma, T., Osaka, T., Saito, M., Mizuno, J., Wada, Y., 2005. Biosens. Bioelectron. 20, 2306–2309.
Huang, Y., Zhang, W., Xie, W., Tang, D., Zhang, H., Du, C., 2013. Sens. Actuators B: Chem. 186, 199–204.
Karakouz, T., Holder, D., Goomanovsky, M., Vaskevich, A., Rubinstein, I., 2009. Chem. Mater. 21, 5875–5885.
Kim, Y.-P., Lee, T.G., 2012. Anal. Chem. 84, 4784–4788.
Ko, S., Park, T.J., Kim, H.-S., kim, J.-H., Cho, Y.-J., 2009. Biosens. Bioelectron. 24, 2592–2597.
LaVoie, M.J., Ostaszewski, B.L., Weihofen, A., Schlossmacher, M.G., Selkoe, D.J., 2005. Nat. Med. 11, 1214–1221.
Lee, H., Dellatore, S.M., Miller, W.M., Messersmith, P.B., 2007. Science 318, 426–430.
Lee, H., Rho, J., Messersmith, P.B., 2009. Adv. Mater. 21, 431–434.
Lee, H., Scherer, N.F., Messersmith, P.B., 2006. Proc. Natl. Acad. Sci. USA 103, 12999–13003.
Li, H., Cui, D., Cai, H., Zhang, L., Chen, X., Sun, J., Chao, Y., 2013. Biosens. Bioelectron. 41, 809–814.
Liu, R., Zhou, J.H., Zhou, Z.K., Jiang, X., Liu, J., Liu, G., Wang, X.H., 2014a. Nanoscale 6, 13145–13153.
Liu, X., Huang, R., Su, R., Qi, W., Wang, L., He, Z., 2014b. ACS Appl. Mater. Interfaces 6, 13034–13042.
Liu, Y., Ai, K., Lu, L., 2014c. Chem. Rev. 114, 5057–5115.
Lynge, M.E., van der Westen, R., Postma, A., Stadler, B., 2011. Nanoscale 3, 4916–4928.
Maisonneuve, M., Valsecchi, C., Wang, C., Brolo, A.G., Meunier, M., 2015. Biosens. Bioelectron. 63, 80–85.
Muench, F., Neetzel, C., Kaserer, S., Broetz, J., Jaud, J.-C., Zhao-Karger, Z., Lauterbach, S., Kleebe, H.-J., Roth, C., Ensinger, W., 2012. J. Mater. Chem. 22, 12784–12791.
Navarrete, M.-C., Díaz-Herrera, N., González-Cano, A., Esteban, Ó., 2010. Plasmonics 5, 7–12.
Perez-Ruiz, E., Kemper, M., Spasic, D., Gils, A., van Ijzendoorn, L.J., Lammertyn, J., Prins, M.W.J., 2014. Anal. Chem. 86, 3084–3091.
Pollet, J., Delport, F., Janssen, K.P., Jans, K., Maes, G., Pfeiffer, H., Wevers, M., Lammertyn, J., 2009. Biosens. Bioelectron. 25, 864–869.
Prodan, E., Radloff, C., Halas, N.J., Nordlander, P., 2003. Science 302, 419–422.
Sciacca, B., Monro, T.M., 2014. Langmuir 30, 946–954.
Sharma, A.K., Jha, R., Gupta, B.D., 2007. IEEE Sens. J. 7, 1118–1129.
Shevchenko, Y., Camci-Unal, G., Cuttica, D.F., Dokmeci, M.R., Albert, J., Khademhosseini, A., 2014. Biosens. Bioelectron. 56, 359–367.
Suzuki, H., Sugimoto, M., Matsui, Y., Kondoh, J., 2008. Sens. Actuators B: Chem. 132, 26–33.
Tabakman, S.M., Chen, Z., Casalongue, H.S., Wang, H., Dai, H., 2011. Small 7, 499–505.
Tu, M.H., Sun, T., Grattan, K.T.V., 2014. Sens. Actuators B: Chem 191, 37–44.
Verma, R., Gupta, B.D., 2015. Food Chem. 166, 568–575.
Wan, Y., Zhang, D., Wang, Y., Qi, P., Hou, B., 2011. Biosens. Bioelectron. 26, 2595–2600.
Wang, Y.X., Ye, Z.Z., Si, C.Y., Ying, Y.B., 2013. Food Chem. 136, 1303–1308.
Wong, W.C., Chan, C.C., Boo, J.L., Teo, Z.Y., Tou, Z.Q., Yang, H.B., Li, C.M., Leong, K.C., 2013. IEEE J. Sel. Top. Quantum Electron. 19 (Article#: 4602107).
Yang, X., Li, J., Pei, H., Zhao, Y., Zuo, X., Fan, C., Huang, Q., 2014. Anal. Chem. 86, 3227–3231.
Zabetakis, D., Dressick, W.J., 2009. ACS Appl. Mater. Interfaces 1, 4–25.
Zangmeister, R.A., Morris, T.A., Tarlov, M.J., 2013. Langmuir 29, 8619–8628.
Zhang, H., Sun, Y., Gao, S., Zhang, J., Zhang, H., Song, D., 2013a. Small 9, 2537–2540.
Zhang, J., Sun, Y., Wu, Q., Zhang, H., Bai, Y., Song, D., 2013b. Analyst 138, 7175–7181.
Zhao, S.S., Bukar, N., Toulouse, J.L., Pelechacz, D., Robitaille, R., Pelletier, J.N., Masson, J.F., 2015. Biosens. Bioelectron. 64, 664–670.
Zhao, Y., Deng, Z.-q, Wang, Q., 2014. Sens. Actuators B: Chem. 192, 229–233.